

Artificial Neural Network for Technical Feasibility Prediction of Seismic Retrofitting in Existing RC Structures

Roberto Falcone^a, Angelo Ciaramella^b, Francesco Carrabs^c, Nicola Strisciuglio^d, Enzo Martinelli^{a,*}

^a*Department of Civil Engineering, University of Salerno, via Giovanni Paolo II n.132, 84084, Fisciano, Italy*

^b*Department of Science and Technology, University of Naples Parthenope, Centro Direzionale - Isola C4, I-80143, Napoli, Italy*

^c*Department of of Mathematics, University of Salerno, via Giovanni Paolo II n.132, 84084, Fisciano, Italy*

^d*Faculty of Electrical Engineering, Mathematics and Computer Science, University of Twente, Hallenweg 19 7522 NH Enschede, Netherlands*

Abstract

The seismic analysis of reinforced concrete (RC) structures generally requires significant computational effort, which can be challenging or at least time-consuming also for the modern computing systems. Particularly, huge computational effort is required for running optimisation procedures intended at selecting the the “best” retrofitting solution among the wide set of technical feasible ones. Therefore, this paper proposes the use of Machine Learning instead of the mechanistic analyses executed as part of an optimisation procedure for seismic retrofitting of RC existing structures recently proposed by the authors. Specifically, an Artificial Neural Network is trained and employed as a possible substitute of finite element analysis for a rapid and accurate assessment of the relevant performance exhibited by the enhanced configurations of an RC existing building typology. The obtained results demonstrate the effectiveness

*Corresponding author.

Email addresses: roberto.falcone@unisa.it (Roberto Falcone), angelo.ciaramella@uniparthenope.it (Angelo Ciaramella), fcarrabs@unisa.it (Francesco Carrabs), n.strisciuglio@utwente.nl (Nicola Strisciuglio), e.martinelli@unisa.it (Enzo Martinelli)

of an artificial neural network as a computational model to approximate a finite element analysis in seismic retrofitting of RC structures by considering several structural configurations. The proposed methodology can be used to speed-up the search of a viable RC strengthening configuration within the whole parametric field of relevance, which can be subsequently refined using more detailed and computationally expensive FE methods.

Keywords: Computational Intelligence, Artificial Neural Networks, Seismic retrofitting, Earthquake engineering.

1. Introduction

Performance-Based Design (PBD) [1] is a well-established approach introduced to overcome the limitations of prescriptive seismic design procedures. It allows engineers to check structures against several performance objectives, not
5 limited to, yet fundamental, human life safety requirement. The set of relevant performance levels in a newly designed building is generally defined by codes and standards [2, 3], but stakeholders (i.e. users, owners, manufacturers) can further raise the design objectives based on various aspects, such as “importance class”, economic considerations, and engineering judgment. Like
10 wise, codes and standards [4] define procedures for assessing vulnerability and designing retrofitting measures for existing buildings. In both cases, seismic analyses have to be executed to estimate the expected structural performance under earthquake actions of variable intensity for each performance level.

The most common structural analysis methods are based on rigorous pro-
15 cedures, based on both mechanical models and numerical methods, such as the well-known Finite Element Method (FEM) [5]. These “mechanistic” simulations of the seismic response of structures are often time consuming and computationally expensive. Hence, when used in iterative design procedures for structural optimisation, they are invoked at every step for the evaluation of the concerned

20 candidate solution, considerably slowing down the design and validation process. This is the case, for instance, of a recently proposed design procedure to select the “cheapest” retrofitting solution on vulnerable reinforced concrete (RC) framed structures [6]: a FEM-based evaluation is performed as fitness function on retrofitting solutions iteratively proposed by a genetic algorithm. 25 In that case, the computation of the FEM algorithm solutions takes the largest part of the computing time, being the bottleneck of the optimization process.

Computational methods have been recently developed to obtain approximate solutions of complex problems in several engineering fields [7], yet requiring significantly shorter computational time than the FEM-based and exact 30 solutions [8]. This class of methods is generally referred at as Computational Intelligence (CI) or Soft-Computing (SC) methods [9], as they are based on heuristic approaches rather than on rigorous or exact physically-based models. Despite an initial scepticism about their actual capability to solve mechanical problems, they were demonstrated to be powerful and applicable to various areas 35 of applied sciences and engineering. A comprehensive review of the main applications of such techniques to relevant structural and earthquake engineering problems has been recently presented [10].

The most popular SC methods are Artificial Neural Networks (ANNs) [11], metaheuristics [12, 13] and fuzzy logic [14]. Recently, deep neural networks, 40 constructed by stacking multiple layers of basic computational units, so called neurons, have reached high popularity. Their capabilities to disentangle highly non-linear relationships in the data or to map complex input-output rules have granted their application in several fields. They indeed became the *de facto* standard to solve problems in computer vision and robotics [15, 16, 17] (e.g. for 45 place recognition [18, 19], scene segmentation and understanding [20, 21], navigation [22]), audio processing (e.g. for music [23] and speech [24] recognition,

multimedia streaming [25]), emotion analysis [26, 27], solar photovoltaic power forecasting [28], among others. Several architectures and types (e.g. multi layer perceptron, convolutional networks, recurrent networks, generative adversarial networks, among others) of neural networks, including deep learning models, have been proposed. They have been recently surveyed in [29]. Besides the comparisons among alternative types of artificial ANN [?], extensive reviews of the literature devoted to the use of ANNs to approach civil engineering problems are available [30, 31]. For instance, they have been used in predicting the linear response of the SDoF system [32], the nonlinear dynamic responses of simple steel [33] or RC framed structures subjected to earthquakes [34], and the simplified “capacity curve” of a given RC building typology [35].

ANNs and computational methods can replace time-consuming conventional procedures employed in many types of problems, such as structural health monitoring and damage identification [36, 37, 38, 39, 40], fragility analysis [41, 42, 43, 44], structural optimisation [? 45] or seismic reliability assessment [46, 47]. However, these studies generally considered simple and newly designed structure, but never the case of existing real-world RC structures in their retrofitted configuration.

This paper is mainly intended at speeding-up the iterative search for the most cost-effective seismic retrofitting solution in existing RC frames. It is based on a neural network used to replace the computationally-intensive FEM-based optimization and provides an approximate solution to the retrofitting optimization problem of a given building, increasing the overall computational efficiency of the design process. Therefore, the proposed network has been incorporated into PBD optimization procedures [6]. It is worth noticing that the proposed network is trained to provide solutions to the retrofitting intervention of a given building. We thus show a prototypical use of the proposed method, which forms the basis

for further development of approaches for design optimization based on efficient
75 computational intelligence techniques. This type of solutions can be deployed to
speed-up the exploration and evaluation of a large number of solutions, obtain-
ing an approximate sub-optimal indications for seismic intervention, which can
be further optimized with exact methods. The benefit of the proposed method
is that the computationally intensive exact methods (e.g. FEM optimization)
80 are used only on a very small sub-set of approximate solutions, thus reducing
the overall design time.

The paper is organized as follows. In Section 2, the existing methodology
for performance-based design for retrofitting interventions is presented, and in
Section 3 the procedures for seismic assessment. In Sections 4 and 5, the basic
85 concepts of neural networks and the model designed for the proposed method-
ology, are respectively described. Furthermore, the results of experiments and
numerical simulations, showing the deployability of the proposed methodology
for optimization of the efficiency of the retrofitting intervention design process,
are presented. Finally, the authors draw conclusions in Section 6.

90 **2. Outline of the Performance-Based Design approach**

Unlike the prescriptive design approach, which evaluates the strength of
the structure at one single performance objective (life-safety), the Performance-
Based-Design (PBD) approach [1] takes into account the performances of the
building after the construction to ensure a reliable and predictable structural
95 response to seismic loading over its lifetime. Two main terms are involved in
this alternative approach: the “performance level” and the “performance objec-
tive”. The former can be described as the extent of damage to structural and/or
non-structural components and it relate to the cost of repairing/restoring the
building to pre-earthquake condition. The latter is the performance required for

100 a given earthquake hazard level represented by the engineering characteristics
of the seismic shaking expected at the construction site (response spectrum, ac-
celerogram, and so on). The main part of a Performance-Based seismic design
procedure is the definition of the performance objectives: they are nothing more
than the combination of one performance level with a specific earthquake haz-
105 ard level. According to the Italian Technical Standards [2], the following four
Limit States (performance levels) are considered: i) Fully Operational Level
(the building does not suffer significant damage and interruption of use); ii)
Operational Level (the damage does not put at risk the users and does not
significantly affect the resistance and stiffness against the vertical and horizon-
110 tal actions); iii) Life Safety Level (the building is subject to serious damage
to structural components associated with a significant loss of stiffness against
horizontal actions but a residual strength for vertical actions); iv) Near Collapse
Level (the building is subject to very serious damage to structural components
with a very small safety margin against collapse for horizontal actions). The
115 ground-shaking hazard is defined using a hazard curve which indicates the prob-
ability that a measure of seismic intensity will be exceeded over a certain time.
Specifically, four seismic hazard levels are considered: i) Frequent Earthquake
with a probability of exceedance equal to 81% in the reference period; ii) Occa-
sional Earthquake with a probability of exceedance equal to 63% in the reference
120 period; iii) Rare Earthquake with a probability of exceedance equal to 10% in
the reference period; iv) Very Rare Earthquake with a probability of exceedance
equal to 5 in the reference period. It's worth to add that the performance ob-
jectives depend on the "importance class" of the structure (see Figure 1): i) for
a basic (standard occupancy) facility four performance objectives are accept-
125 able (B1, B2, B3, B4); ii) for an essential facility three performance objectives
are acceptable (E1, E2, E3); iii) for a safety-critical facility two performance

objectives are acceptable (SC1, SC2).

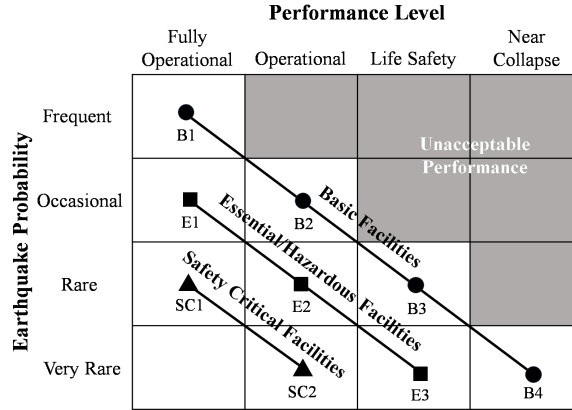


Figure 1: Performance objectives depending on the facility type and purpose [1].

3. Seismic assessment

Defined the performance objectives, the seismic analysis of the building has
 130 to be executed to determine its performance level in a given earthquake scenario.
 The PBD approach generally implies the use of displacement-based non-linear
 (pushover) analysis able to accurately simulate the level of damage it is ex-
 pected to occur as a result of the “excursion” in the non-linear range of the
 response. The seismic structural performance point (PP) is usually obtained
 135 through the Equivalent SDoF Method (or N2-Method) proposed by Fajfar [48],
 which provides a clear graphical representation of how a building behaves under
 an earthquake ground motion. It locates the PP at the intersection between the
 Inelastic Demand Response Spectrum (IDRS) and the bilinear Capacity curve
 of the structure obtained through a pushover analysis (Figure 2).

140 Consistently with PBD framework, structural behaviour is assessed in multi-
 ple hazard levels of increased intensity. Hence, engineers are called to carefully
 examine the results of such analyses in order to take one of these decisions:

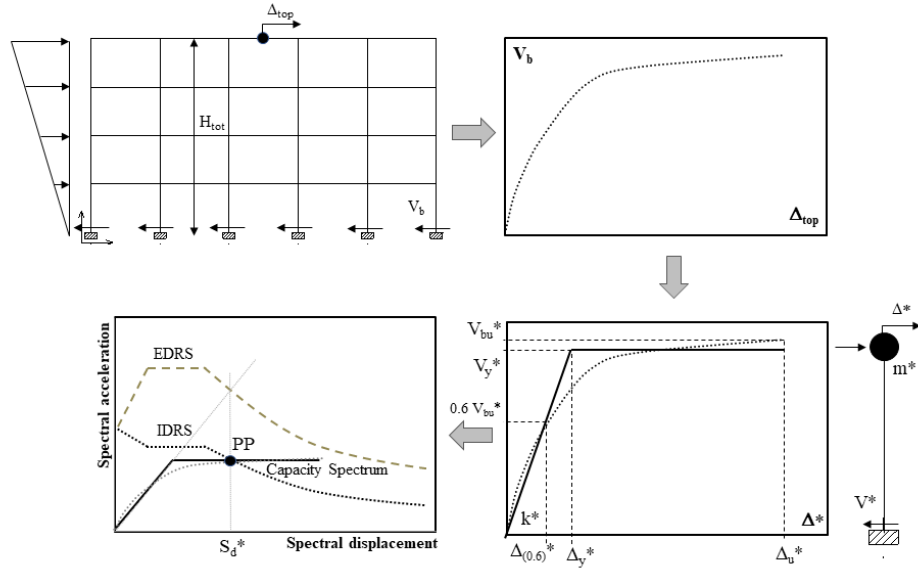


Figure 2: Conceptual steps for the application of the N2-Method.

a) propose the repair and maintenance of the building; b) design a seismic retrofitting intervention; c) declare the building unfit for use and to be demolished.

3.1. Seismic retrofitting

It is highly likely that an existing building in a earthquake-prone area does not meet the performance requirements mainly due to its high vulnerability, namely the susceptibility to damage induced by an earthquake of a given magnitude. Regarding the RC structures, the vulnerability mainly depends on the deficiencies that can be broadly classified as local (deficiencies in individual members) and global (deficiencies which are observed in the structure as a whole). The former typically include the poor detailing of single structural members or connection between them, poor-quality materials, and so on. The latter control the degradation of the lateral load-resisting mechanism of a building subjected to an earthquake. A seismic retrofitting strategy aims at effectively reducing

these deficiencies and increasing the performance level of an existing building to the desired objective. From a mathematical standpoint the purpose of a retrofit program is to meet the following inequality:

$$g_{LS} = C_{LS} - D_{LS} \geq 0 \quad \forall LS = 1 \rightarrow n_{LS} \quad (1)$$

160

where the term C_{LS} is the available Capacity of the structure at the n_{LS} Limit States under consideration and the term D_{LS} is the corresponding Demand at the same Limit State. Capacity and Demand can be intended in terms of both displacement (for ductile mechanisms of damaging) and forces (for brittle mechanisms of damaging). An engineer can try to meet this inequality by two main strategies: a) improving the dynamic capacity of the existing building (increasing the strength, the stiffness, the deformation capacity of individual members) or b) decreasing the seismic demand (increasing the period of vibration, increasing of damping factor, reducing the reactive mass, changing the intended use).

170

On the one hand, when the building is found to be severely deficient under seismic forces, the first attempt in a seismic retrofit program is usually a global intervention intended at decreasing the displacement demand on the existing structural and non-structural components [49]. The most common global interventions are based on either base isolation system, installation of dissipative devices, addition of RC walls, the addition of infill walls, or steel bracing systems. On the other hand, if the number of elements found to be inadequate to their function is not excessive, the group of local interventions including reparation, reinforcement, or replacement of individual structural elements is usually preferred. However, they are inappropriate to significantly modify the overall behaviour of the structure, meaning the lateral strength or the stiffness. The

180

member-level techniques fall under three different types: concrete jacketing, steel jacketing, and fiber-reinforced polymer (FRP) sheet wrapping [50]. Since it is possible to obtain an high number of different retrofitting solutions, the rational choice of the most suitable one needs to take into account a series of concurrent criteria within the framework of a Multi-Criteria Decision process [51]. Such criteria can be based on both strictly quantitative measures, such as specific parameters related to the seismic response of the retrofitted structures [52] and the life-cycle cost [53], or qualitative measures, such as the users opinion or aesthetical aspects [54]. Surely, an initial selection can be done by distinguishing the technical solutions that satisfy the constraints given in the inequality (1) from the others: they can be labelled as “feasible” and “unfeasible”, respectively.

4. Artificial Neural Networks

Artificial Neural Networks (ANNs) are Computational Intelligence methodologies, originally inspired by neuro-physiological findings about the structure and functions of the human brain, composed of interconnected processing units that implement capabilities such as learning from experience [11], generalizing from previous examples, and abstracting essential characteristics from sets of inputs containing irrelevant data. In pattern recognition problems, ANNs are used to classify input feature vectors into a set of target categories. In fitting problems, they are used to find a mapping between a data set of numeric inputs and a set of numeric targets. The basic computational units are called “artificial neurons” and transform the input via a weighted linear combination operation [55]. It receives input a set of signals (x_1, x_2, \dots, x_m) from m neurons at the preceding layer of the network architecture and it transforms them into an output signal (y_k) by weighted linear combination (with weights assigned

to the input synapses) followed by an activation function f . The input signals are introduced to neurons through their synapses, multiplied by the respective synaptic weights ($w_{k1}, w_{k2}, \dots, w_{km}$), and are added algebraically together with the bias by an adder. Formally, the linear combination of the inputs of a neuron is defined as:

$$u_k = \sum_{j=1}^m u_{kj} \cdot x_j + b_k \quad (2)$$

The activity u_k becomes the argument of an activation function $f(u_k)$ which introduces non-linearity in the estimation of the model. Different types of activation functions can be used, e.g. the sigmoid, hyperbolic tangent, softmax, linear, threshold. The model of an artificial neuron is shown in (Figure 3).

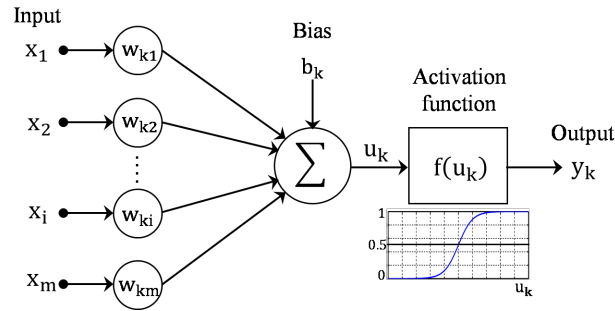


Figure 3: Model of a single artificial neuron [37].

The architecture of a ANN consists of a specific number of layers, each one composed of several neurons and an activation function. One of the most used architecture is the Multi-Layer Feed-Forward Neural Network (MLFFNN) or Multi-Layer Perceptron (MLP), composed of an input layer, several hidden layers, and an output layer. In these networks, the neurons in any layer are connected to all neurons in the adjacent layer (fully connected networks, see Figure 4 for an example of its topological structure).

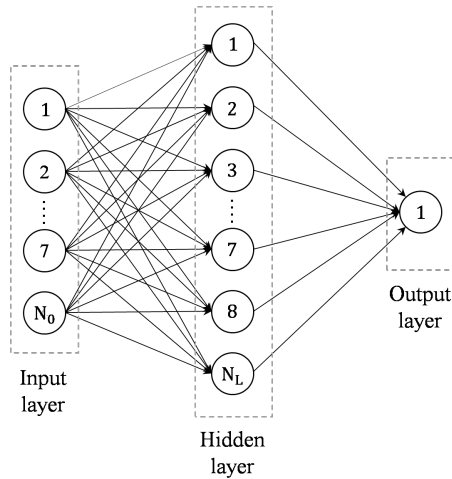


Figure 4: Typical Multilayer Feed-Forward perceptron ANN.

225 An ANN consists of nonlinear activation functions and a set of model parameters (synaptic weights \mathbf{w} and biases \mathbf{b}). The initial weights are set to a random small value chosen between -0.5 and $+0.5$, and then they are adjusted to minimize the difference between the ANN predictions and the targets, summed over every training example. The aim of the learning algorithm is, hence, to determine an optimum set of the weight parameters \mathbf{w} by minimizing a loss function
 230 computed on the output. In the literature there are several learning algorithms: Levenberg-Marquardt [56], Scaled Conjugate Gradient [57], Quasi-Newton [58], Resilient Backpropagation [59], among others.

For the training and evaluation of the proposed network, a cross-validation
 235 protocol is used, dividing the data set into 3 independent subsets: a) training subset, which is used to determine the optimal weights \mathbf{w}_* that minimize the error function of the model; b) validation subset, which supervises the training process; c) test subset, which is used afterward to evaluate the generalization capacity of the trained ANN model. The training automatically stops when the
 240 generalization is no more improved, as indicated by an increase of the cross-

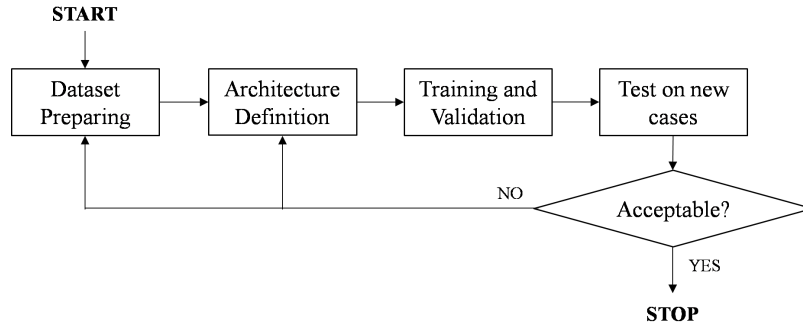


Figure 5: Flow-chart of the Neural Network scheme.

entropy error for classification problems, or of the mean square error of the validation samples for problems.

5. The proposed neural network meta-model

This work mainly aims to propose a NN-based meta-model for the estimation of the seismic response of real-world RC strengthen structural systems for multiple hazard levels at an affordable computational time. More specifically, the present study aims to propose a MLFFNN able to classify the input vectors that describe the retrofitting intervention as “feasible” or “unfeasible”. The procedure to train the ANN consists of the following steps: 1) preparation of the data set; 2) definition of the NN architecture; 3) feature selection and normalization; 4) ANN training and validation; 5) test of the trained ANN on new retrofitting solutions. The flow-chart of the procedure is shown in Figure 5.

5.1. Dataset pre-processing

ANNs are able to learn and generalize from examples belonging to an existing dataset. In this section, the procedure followed to generate an adequate number of $[input-output]$ pairs, to be employed as examples for the ANN training, is presented. This procedure consists of two steps: structure modelling and numerical simulation.

5.1.1. Structure modeling

260 The structure modelling consists of establishing a set of mathematical partial differential equations to describe the mechanical behaviour of the underlying model. In this paper, structural analyses are run in OpenSEES [60], but the proposed procedure can ideally be implemented through whichever software for seismic simulation of structures. The case study employed to demonstrate the
265 potential of the proposed ANN scheme refers to an RC residential building obtained through simulated design according to the practices and techniques in force in Italy during the 1970s. The selected four-storied structure is regular in plan and elevation (according to the criteria set by EC8 [3]). The long side, the short side, and the inter-story height are respectively equal to 25.00 m, 15.00
270 m, and 3.50 m. The permanent load is $G = 5.00 \text{ kN/m}^2$ and the live load is $Q = 2.00 \text{ kN/m}^2$. Gravity loads are applied to an effective area of 375 m^2 . The seismic mass of the first three floors is $W_1 = W_2 = W_3 = 3500 \text{ kN}$, while the seismic mass on the fourth floor is $W_4 = 2900 \text{ kN}$.

The uniaxial Kent-Scott-Park model [61] with degraded linear unloading/reloading stiffness and no tensile strength has been assumed for modelling
275 the behaviour of concrete in the as-built configuration. Reference has been made to a resistance class C20/25. A bilinear stress-strain curve has been adopted for describing the elastic-plastic behaviour of steel: the modulus of elasticity of steel has been chosen equal to 210 GPa and the yield stress F_y is 220 MPa.
280 The cross-section of RC members has been discretized into fibers that comply with beam kinematics and each follows its constitutive stress-strain response whose integration defines the stress resultant force-deformation response at a beam-column sample point. More specifically, the rectangular RC sections are composed of patches (groups of fibers): 4 cover concrete patches, 1 core concrete
285 patch, and 3 reinforcing layers of longitudinal rebars (top, bottom, and interme-

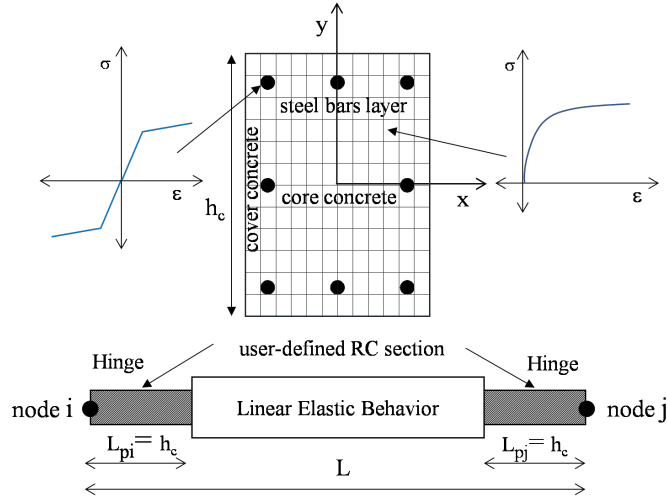


Figure 6: Plastic hinge model adopted in the FEM model of RC members under consideration.

diate skin reinforcement layers). The core concrete patch has been considered to be not confined by the transversal stirrups (due to their wide spacing) and it has been discretized into 100 fibers. The plasticity has been assigned at the end element in the so-called “plastic-hinge” region with a finite length L_p , while
 290 the central part of the beam has been simulated by a linear elastic element as shown in Figure 6. In the present work, the plastic hinge length L_p has been chosen to be equal to the cross-section’s height of the element.

The floor, which is one of the most important elements for the distribution of seismic actions, has been schematized with diagonals members made of a
 295 linear elastic material (with Young Modulus E) because it cannot be considered infinitely rigid in its plane. To this end, truss elastic elements hinged at the ends have been used. In the present work, the axial stiffness of diagonal truss is based on a reliable and widespread formula available in the literature [62]. The whole frame has been assumed to have rigid joints for simulating beam-to-
 300 column connections. Foundation has not been simulated, but the building has been considered to be fully fixed to the ground. Non-structural elements have

not been included in the FE model. It is worth highlighting that this FE model representing the as-built condition has been verified to not meet the inequality in all the seismic scenarios described in the following Section. Hence the existing
305 structure requires a seismic retrofit intervention.

The intervention type considered in this work is a global intervention realized by installing X-shape concentric steel bracings. In order to quickly generate a large dataset of examples, a simple encoding rule has been established to describe the retrofitting interventions. The steel bracings have been supposed
310 to be possibly realized between each couple of columns connected by a beam. However, since the structure under consideration is regular in elevation and with a symmetrical plan, it has been assumed that even the global interventions are symmetrical, to not alter its regularity. As a consequence, the number of design variables X_i (input parameters) strictly necessary for describing the
315 global stiffening intervention (10 variables) is less than the total number of beams on the first floor (32 beams) shown in Figure 7. As shown, the beams involved for the symmetrical interventions have been highlighted with the same color. This leads to having each bracing described by only one steel profile, which is quite convenient to keep the cardinality of the input vector X as small
320 as possible.

The design variables X_i point to a position in a commercial steel profile table containing a list of available commercial H-shaped sections with their relevant geometric properties. Each variable describes the section of diagonals possibly installed at the first story in correspondence of a specific beam (Figure
325 8): it can assume an integer value ranging between 0 (i.e. absence of bracing system) and 7 which represent the row (label) in the table: the greater the integer number, the larger the cross-section required for realizing the global intervention. Such information has been employed for modifying the Finite

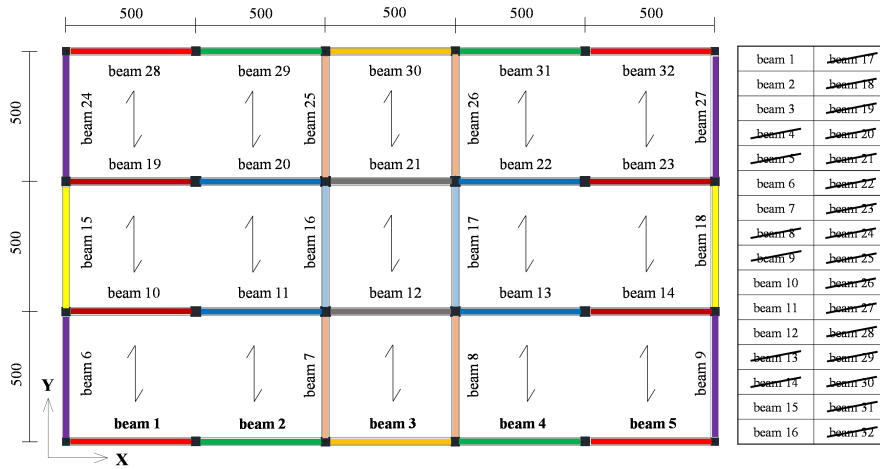


Figure 7: First-floor plan of the existing structure.

Element Model of the as-built structure: a new lateral-force-resisting system
 330 composed of bracing members, with a specific topology and section, is added to
 the existing RC frame.

To this end, a force-based spread plasticity element has been used. Specifi-
 cally, a “fiber section model” has been considered to distribute steel inelasticity
 through the cross-sections and along the bracing member length [63]. Each
 335 bracing element has been discretized into five H-shaped cross-sections located
 at the Gauss-Lobatto quadrature integration points: two integration points at
 the element edge and three in the middle (Figure 9). Each section has been
 subdivided into a grid of “fiber”, each of them associated with the uniaxial
 stress-strain constitutive law of the steel material. In particular, the web and
 340 the flange have been considered discretized into 10 fibers.

Moreover, since the concentric X-shaped steel bracing has been modelled
 with four elements whose length is one half of the diagonal, an accidental ec-
 centricity has been assigned to the “middle point” (out of the plane where the
 bracing system lies) according to EN 1993-1-1 [64] for simulating the buckling

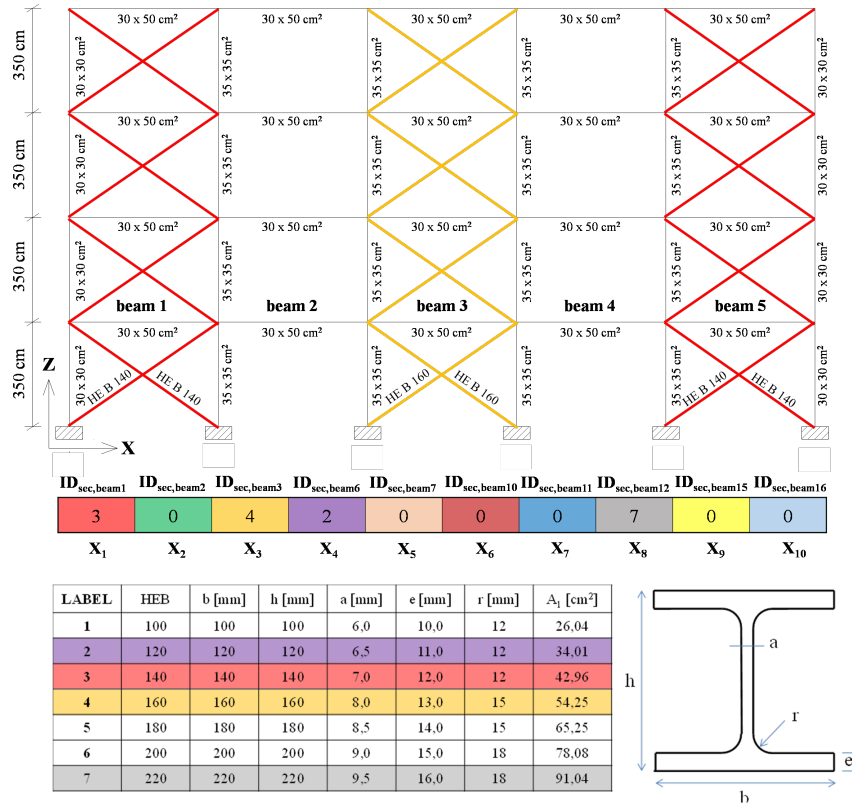


Figure 8: Input variables describing the concentric steel bracings.

345 effects in the compressed elements. The area of the cross-section of steel members has been supposed to decrease with the height in the same way as the shear plan. A consistent design relationship has been assumed between the section of steel members at the first level and the section of steel bracing members at upper levels. Nevertheless, the entire design space consists of 108 different global stiffening solutions. To select input vectors representative of the multi-dimensional design space, a random sampling has been chosen. It is worth noting that each input vector can be ideally “replaced” by its mono-dimensional version. Each input vector can be associated with the numerical result of the summation operator applied to its design variables, as shown in Figure 10.

350

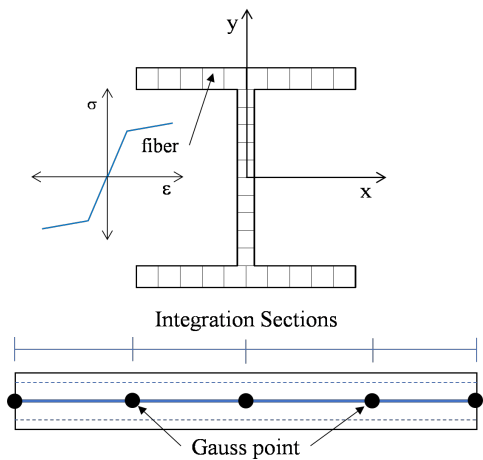


Figure 9: Fiber section model used for the bracing members.

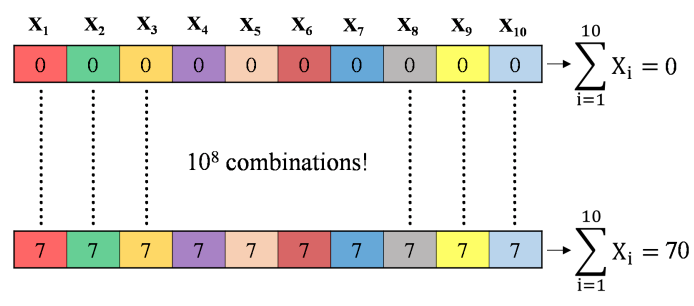


Figure 10: Mono-dimensional representation of the design space

355 A function has been implemented in Matlab [65] for the purpose: it takes
as input a summation value selected in the range [0–70] and it returns one
of the possible input vector characterized by that value. For each one of the
possible 70 summation values, 30 variables array have been randomly generated.
Therefore, a set of 2100 retrofitted configurations have been generated. Such
360 configurations differ from each other in the topology and cross-section size of
the bracing systems added to the 3D frame.

5.1.2. Numerical simulation

The second step of the training data set preparation consists of a set of numerical simulations necessary to determine a reliable target class of the retrofitting intervention modelled in the previous step. The numerical resolution method chosen in this work for simulating the building response is the Finite Element Method [5]. For the present investigation, two seismic intensity levels against which to evaluate the performance have been considered: occasional (Figure 11) with a return period of 50 years and rare earthquakes (Figure 12) with a return period of 475 years, according the Italian standard code [2]. Moreover, three different construction sites have been taken into account to cover a wide domain of real cases: Site 1 (low level of seismic hazard); Site 2 (middle level of seismic hazard), and Site 3 (very high level of seismic hazard). The engineering characteristics of the seismic shaking expected at the construction site have been represented through the Elastic Response Demand Spectra (ERDS). According to the Italian Code [2], the parameters needed to describe the branches of the ERDS depend on the seismic hazard level which is based on the geographical coordinates of the construction site, the nature of subsoil/soil and nominal life of the building and its “importance class”.

The seismic parameter, selected in the present work to represent the magnitude of the seismic shaking, is the spectral acceleration at the plateau branch of both EDRS. Such parameters have been included in the array of input variables along with the design variables encoding the retrofitting intervention. Since the 2100 retrofitting interventions have been assumed to be installed on an existing building supposed to be built in each of the three construction sites, a total of 6300 training examples have been obtained from this combination.

The target labels whereas must be defined with a good degree of approximation so that the resulting ANN-based meta-model could be reliable. Hence,

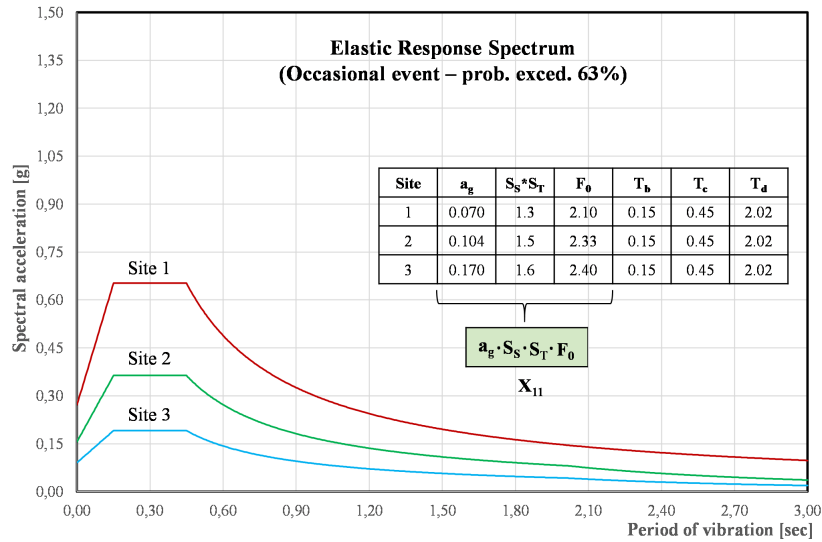


Figure 11: Input variable representing "occasional" seismic events

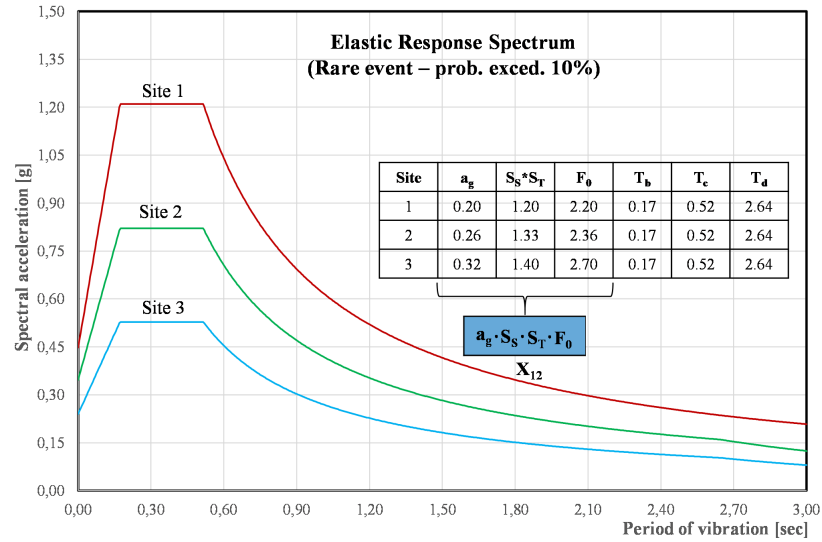


Figure 12: Input variable representing the "rare" seismic event

the performance exhibited by the building in its retrofitted configurations have
 390 been analysed through Nonlinear Static (Pushover) Analysis which nowadays
 have widespread applicability in the field of assessment of existing first mode

dominated building [66]. This type of analysis can accurately simulate the in-elastic deformations (i.e. the damage status), although they require neither ac-celerometric signals nor complex stress-strain relationships under cyclic actions.

395 Such a procedure is intended at determining a capacity curve which provides the simplified trend of the equivalent lateral global force as a function of the lateral displacement of the structure in a control node, when a system of inertial forces is applied and increased proportionally until collapse. In this preliminary ap-plication, only a lateral load distribution with an inverted triangle (first mode)

400 shape has been considered (Figure 13). This is intended at reproducing the so-called “modal” distribution of lateral loads foreseen by EN 1998-1-1:2004, since the first vibrating mode dominates in the dynamic of the considered structure (regular in plan and in elevation). Moreover, the response has been investigated in the main orthogonal stiffness directions: for each retrofitting solution, two

405 pushover analyses have been carried out and the response of the control node was monitored both in X and Y direction. A target displacement equal to 3% of the total height of the structure is sought while the displacement step of the incremental analysis is set to 1% of the target displacement.

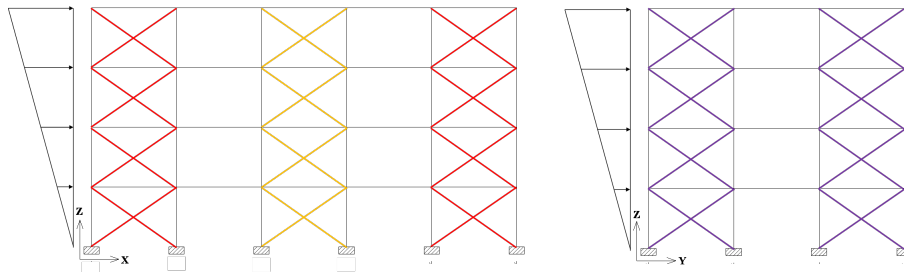


Figure 13: Lateral load distribution assumed in the pushover analyses

Likewise, in the post-simulation phase the Limit State function $g_L S$ has been

410 evaluated at two performance levels and two seismic directions in order to check the technical feasibility of the seismic retrofitting intervention conceptually de-

scribed in the inequality (1).

On the one hand, for the calculation of the seismic capacity C_{LS} three assumptions have been made: 1) the inter-story demand drifts δ_D have been
415 considered herein as damage index; 2) the drift capacity δ_C of frame elements at Operational Level (i.e., “SLD” according the Italian Code definition) and Life Safety Level (i.e. “SLV” according the Italian Code’s definition) have been defined in terms of chord rotation at yielding θ_y and collapse conditions θ_{um} , respectively [67] 3) a biaxial interaction domain of the drifts has been consid-
420 ered to take into account the deflections in both X and Y directions and to find the pushover step at which the performance levels (the seismic Capacity $C_{LS,i}$) are achieved. On the other hand, the maximum displacement demand $D_{LS,i}$ for the strengthening structure has been estimated with the N2-Method [48]. The so-called “performance point” of the equivalent SDoF system has been
425 assumed as the intersection point between the bilinear Capacity Spectrum (obtained from the pushover curve) and the Inelastic Response Demand Spectrum (obtained from the Elastic Response Demand Spectrum scaled by the reduction factor R_* of the SDoF system). As the last step of N2-Method, in the post-processing phase the inelastic displacement demand of the equivalent SDOF
430 system $S^*_{d,max}$ has been converted to the global inelastic displacement demand of the original Multi-Degree-of-Freedom system through the modal participation factor. As both capacity and demand terms are known, the Limit State function g_{LS} can be evaluated in both performance levels and seismic directions.

The training data set consists of: (a) 6300 training vectors x whose dimen-
435 sion is 1×12 (the 10 structural parameters chosen to describe the retrofiting intervention and the 2 seismic variables representing both the rare and occasional expected earthquake); (b) 6300 target vectors whose dimension is 1×4 (the 4 values of the $g_{LS,i}$ obtained from the pushover analyses conducted). For

INPUT												TARGET SLD-X		TARGET SLV-X		TARGET SLD-Y		TARGET SLV-Y	
X_1	X_2	X_3	X_4	X_5	X_6	X_7	X_8	X_9	X_{10}	X_{11}	X_{12}	$g_{SLD,X}$	CLASS	$g_{SLV,X}$	CLASS	$g_{SLD,Y}$	CLASS	$g_{SLV,Y}$	CLASS
2	0	3	4	0	1	6	2	7	0	0.19	0.53	> 0	1	< 0	0	> 0	1	< 0	0
4	1	0	2	5	3	0	3	1	4	0.19	0.53	< 0	0	< 0	0	> 0	1	> 0	1
5	3	5	0	3	6	1	2	0	0	0.19	0.53	< 0	0	> 0	1	< 0	0	< 0	0
0	2	7	4	2	0	5	2	7	2	0.19	0.53	> 0	1	> 0	1	> 0	1	> 0	1

Figure 14: Definition of the target classes for each input vector

each input vector belonging to the training dataset, a binomial classification has
440 been done on the basis of the following classification rule: if the value of Limit
State function is positive the numeric class is 1, otherwise the numeric class is
0, as shown in Figure 14. It is easy to see that only if the four values of $g_{LS,i}$
are greater than zero the corresponding seismic retrofitting intervention can be
labelled as feasible. On the contrary, even if only one of these values is negative,
445 the corresponding input vector has to be classified as unfeasible. The size of
the feasible and unfeasible sub-sets is equal to 52% and 48% of D , respectively.
Hence, a well-balanced dataset has been obtained.

5.2. MLP architecture

The adopted MLP model is composed by one input layer, one single hidden
450 layer and one output layer. We stress that this model has universal approxi-
mation properties avoiding in our experiments the use of deep NNs [68]. The
input layer is composed by 12 neurons: 10 neurons are fed with the informa-
tion about the retrofitting intervention and 2 nodes with the Elastic Design
Response Spectra. The input values have been normalized to the range $[0, 1]$,
455 to guarantee that feature values deriving from different measurements can be
effectively compared and the network can weight the features properly, avoid-
ing dominating features [69] [70]. Normalization also contributes to speed-up
convergence of training.

A single hidden layer has been deployed, considering that the efficiency of

460 such an ANN architecture has been well-documented in numerous relevant studies (i.e., universal approximation) [71] [72] [73]. Furthermore, by deploying more hidden layers, we did not observe substantial performance differences. Using a single hidden layer thus contributes to achieve high performance while keeping the computational load contained, which is one of the aims of the present work.

465 The selection of the number of neurons in the hidden layer, whereas, is a trial and error process and it generally starts by choosing a network with a small number of hidden layers and hidden neurons [74]. A grid search approach is adopted for selecting the number of nodes in the hidden layer. The number of hidden neurons has been assumed to range between 10 and 50 (Figure 15)(we

470 used the Neural Net Pattern Recognition app of the Deep Learning Matlab Toolbox [75]).

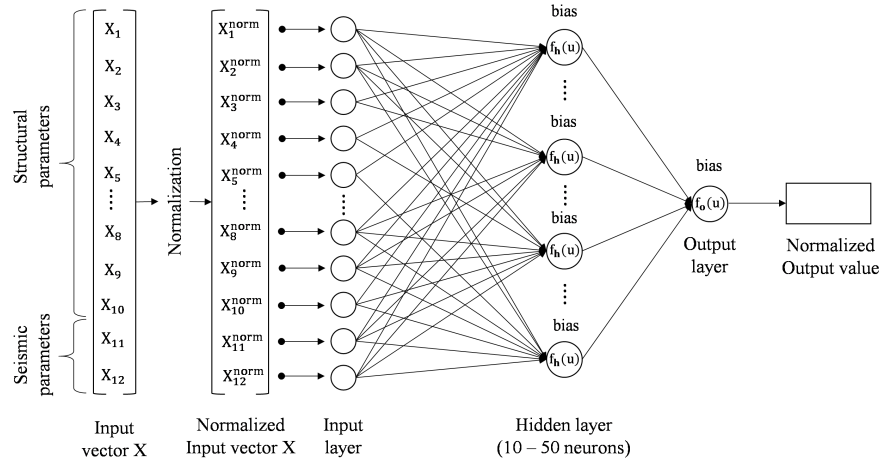


Figure 15: General configuration of the proposed s.

Since the predictions of the Limit State function for each performance level and each seismic direction can be seen as four “independent” problems, an equal number of fully connected ANNs have been built (Figure 16).

475 Hence, for each net, a single output node has been used to represent the

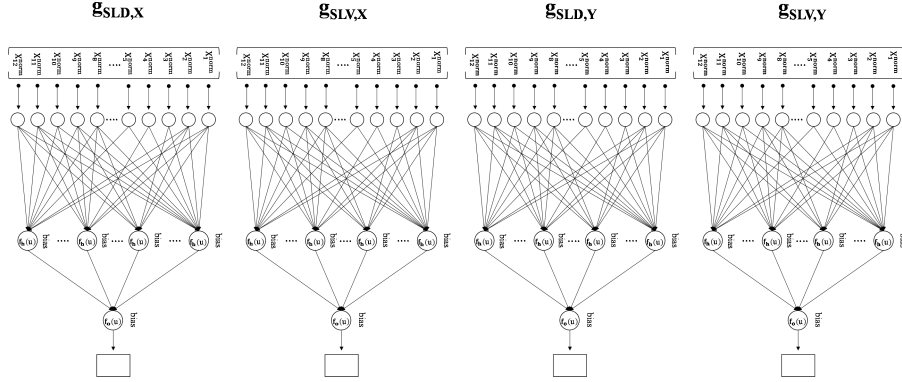


Figure 16: Decoupling of the classification problem through four ANNs.

target class of the retrofiting intervention corresponding to a specific Limit State and seismic loads direction. Moreover, a sigmoid (logistic) activation function f_h has been used for the hidden layer neurons. Instead, for the output neuron a softmax activation function f_o , used in most multi-class or binary classification methods in which the output quantity attains a scalar value $[0, 1]$, has been chosen. It is worth say that this scalar corresponds to the calculated probability of the class. Therefore, the normalized output values between $[0, 0.5]$ have been interpreted as 0 class (i.e. $g_{LS} < 0$), while the values between $[0.5, 1]$ have been interpreted as 1 class (i.e. $g_{LS} > 0$), as depicted in Figure 17.

5.3. Training and validation

For the A training a cross-validation approach has been adopted. The partition of the data set D is obtained by Neural Net Pattern Recognition app at random [75] to ensure good generalization of networks and to avoid overfitting during the training [76] [77]. For obtaining the generalization properties of the model we considered a K-fold cross-validation approach (in particular leave-one-out ($K = 1$)) [78] as described in Figure 18.

For weights update four learning algorithms have been considered: the Levenberg- Marquardt (LM) algorithm [56], the Scaled Conjugate Gradient al-

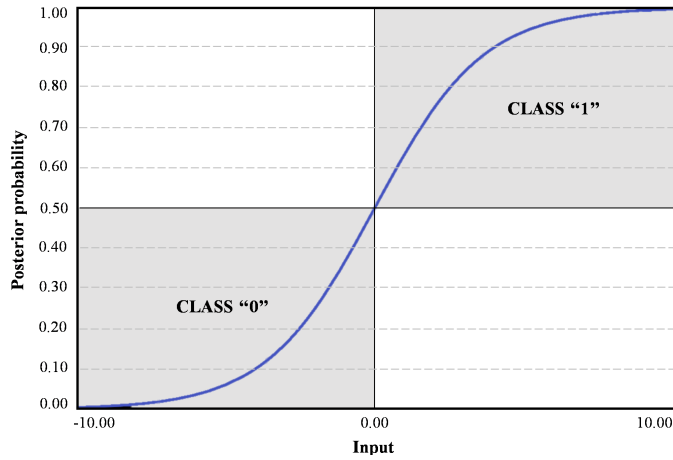


Figure 17: Interpretation of the scalar output of the softmax activation function.

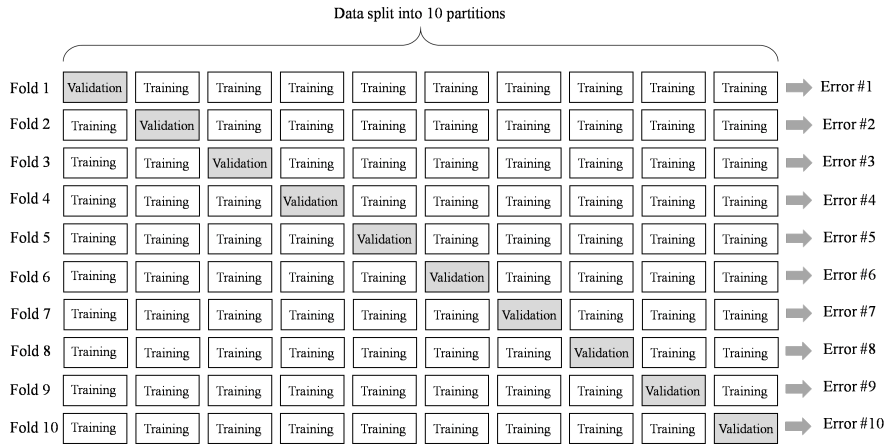


Figure 18: K-fold validation approach.

algorithm [57], the Quasi-Newton algorithm [58] and the Resilient Backpropaga-
 495 tion algorithm [59]. The selection of the training algorithm and the definition of
 the number of hidden neurons has been approached as an optimization problem:
 the architecture and the algorithm that show the highest predictive accuracy
 after the cross-validation have been chosen for the final metamodel, where the
 accuracy is the ratio of number of correct predictions (i.e. the sum “true feasi-
 500 ble” + “true unfeasible”) to the total number of input samples. Although the

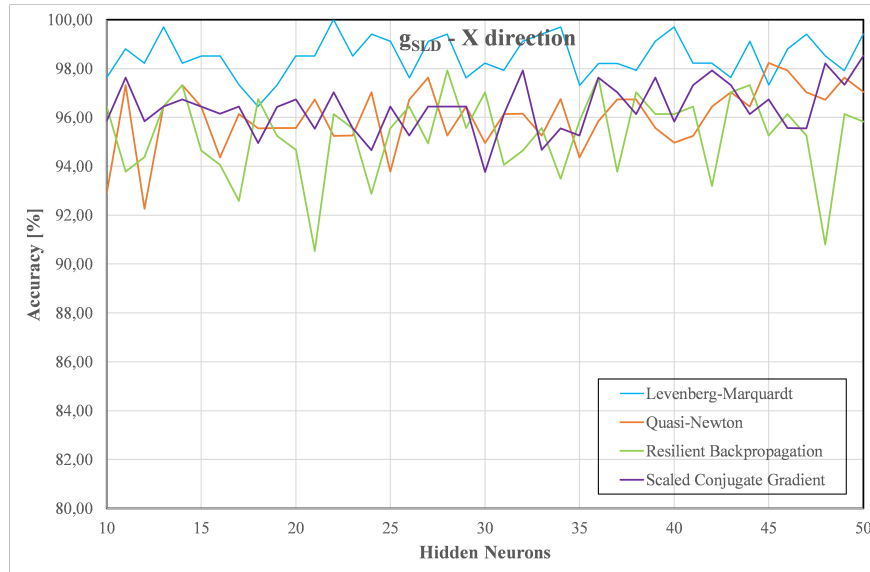


Figure 19: Influence of the training algorithm and hidden neurons on the accuracy for $g_{SLD,X}$.

Figures 19-22 clearly show that the LM algorithm returns the best results in the four cases, the influence of the hidden neurons on the accuracy appears less clear. For simplicity, a unique hidden neurons number equal to 30 has been set for the four neural networks.

505 *5.4. Test*

In order to assess the performance of the trained meta-model, a large set of test examples has been considered. 1500 different retrofitting configurations (with respect to the examples contained in the training dataset) of the same existing RC frame described in Section 5.1.1, assumed to be built in new construction site, have been generated with the aim to predict their technical feasibility with the proposed artificial A-based classifier. What distinguishes the 1500 new examples from the 6300 already used is certainly their “vectoria” representation which is characterised by different values for both variables X_11 and X_12 . The EDRS representative of the seismic intensity expected on the construction

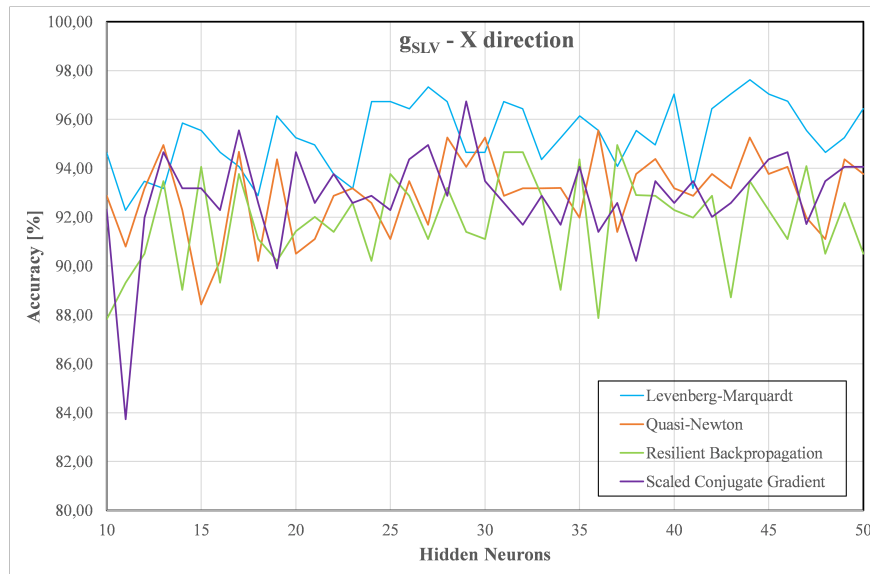


Figure 20: Influence of the training algorithm and hidden neurons on the accuracy for $g_{SLV,X}$.

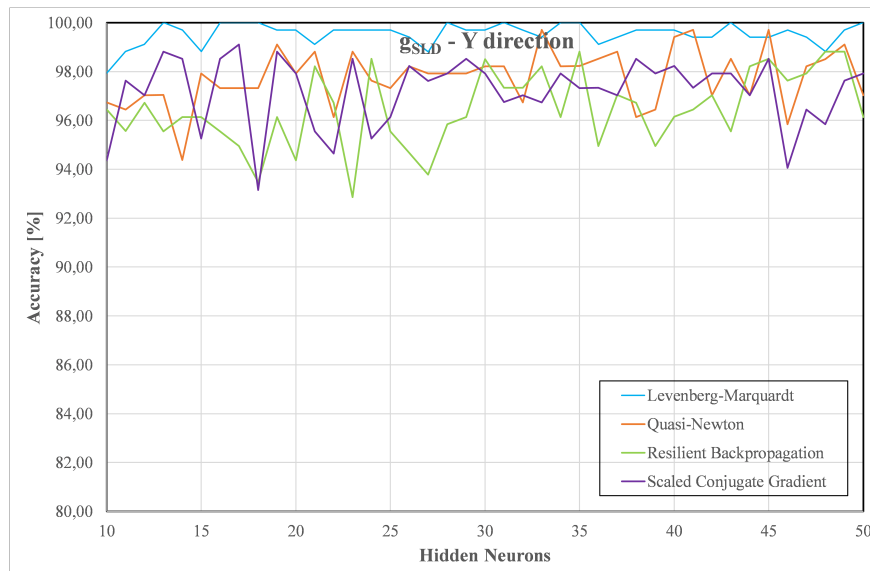


Figure 21: Influence of the training algorithm and hidden neurons on the accuracy for $g_{SLD,Y}$.

515 sites is depicted in Figures 23-24. It has been selected in the middle of two EDRS, respectively of site 1 and site 2, with the aim of “distancin” as much as

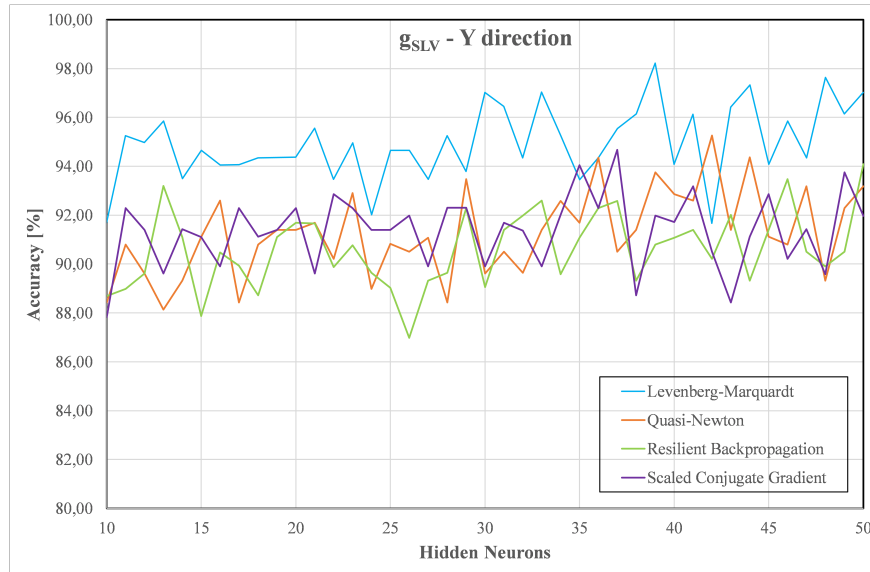


Figure 22: Influence of the training algorithm and hidden neurons on the accuracy for $g_{SLV,Y}$.

possible the cases used for the test from those already used for training.

For each of the 1500 retrofitting configuration the predicted and the true class have been obtained respectively with the ANN-based classification and the pushover analysis in OpenSees. The results achieved with the proposed meta-model, compared with those of the FInite Element simulation, are shown in a confusion matrix: the diagonal and off-diagonal cells correspond to correctly and incorrectly classified observations, respectively. It is worth remembering that the overall class of the generic intervention is the product of the four outputs of the binomial classification (see Section 5.1.2). Since the overall error of the artificial ANN-based meta-model is affected by the misclassification of the four decoupled neural networks, the accuracy of the artificial classifier has been investigated also in each load direction (X and Y) and each performance level (SLD and SLV).

As can be seen in Figure 25, according to the OpenSees results the test dataset includes 1192 technically feasible intervention and 308 unfeasible inter-

ventions. The ANN has recognized 82, 31% of the first group and 75, 91% of the second group. In this work the labels “feasible” and “unfeasible” have been used not only to classify the retrofitting intervention according the lowest values assumed by the limit state function g_{LS} among the 4 combinations (SLD-X; SLV-X; SLD-Y; SLV-Y) but also to categorize the intervention according the minimum values of g_{LS} : a) in X direction (SLD-X; SLV-X), b) in Y direction (SLD-Y; SLV-Y), c) at SLD limit state (SLD-X; SLD-Y), d) at SLV limit state (SLV-X; SLV-Y). As can be seen in Figure 26, the ANN has recognized 91, 12% of the (1249 true cases) “feasible” interventions and 70, 52% of the (251 true cases) “unfeasible” ones in X direction. As regards the Y direction, whereas, the ANN has “recognized” 82, 31% of the (1431 true cases) “feasible” intervention and 75, 91% of the (69 true cases) “unfeasible” ones (see Figure 27).

As can be seen in Figure 28, the ANN has “recognized” the 93, 90% of the (1331 true cases) “feasible” interventions and the 58, 96% of the (169 true cases) “unfeasible” ones at SLD limit state. As regards the SLV limit state, whereas, the ANN has “recognize” the 84, 47% of the (1205 true cases) “feasible” intervention and the 66, 49% of the (295 true cases) “unfeasible” ones (see Figure 29).

5.5. Deploy of the ANN

To better appreciate the advantage of using such neural network, it has been further tested within the context of a rational procedure shown in Figure 30, based on the application of Genetic Algorithms and intended at selecting the “cheapest” retrofitting solution among the technically feasible ones [6]. More specifically, the mapping capabilities of the proposed ANN-based meta-model have been incorporated into an highly demanding PBD optimization procedure whose computational cost is one of the main critical issues to be addressed in order to become actually feasible in real applications.

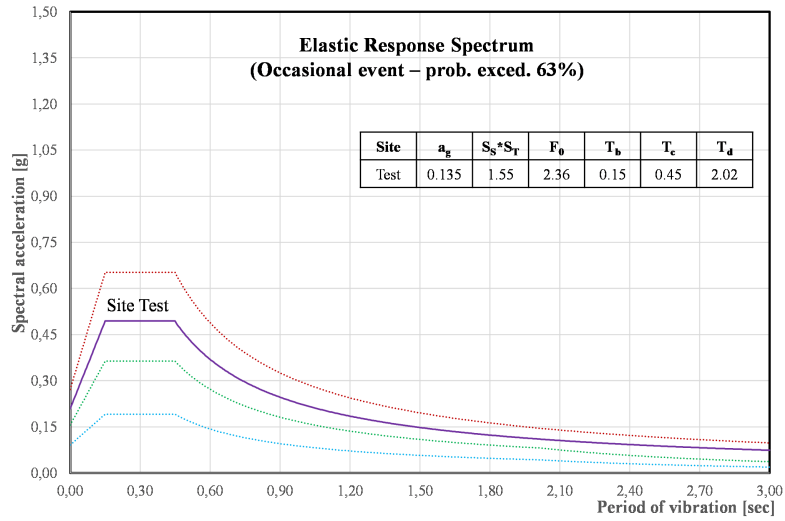


Figure 23: EDRS for an occasional event expected at the site “test”.

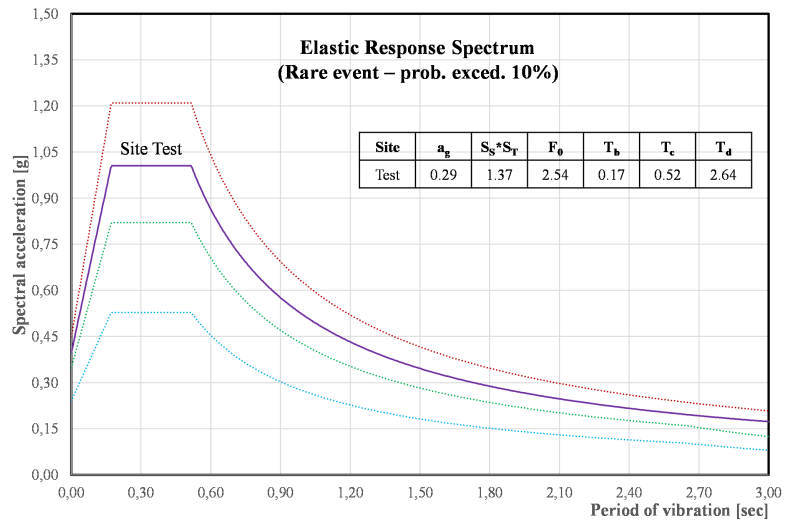


Figure 24: EDRS for a rare event expected at the site “test”.

The proposed ANN-based model is used as an approximate substitute of
 560 a computationally expensive finite-element-based optimization procedure. The
 configuration of the design pipeline is used with the proposed neural network
 (see Figure 31) to explore the space of possible solutions in a time-efficient way

		Predicted Class (ANN)		
		Feasible	Unfeasible	
True Class (OpenSees)	Feasible	True Feasible 981 (82,31%)	False Unfeasible 211 (17,69%)	1192
	Unfeasible	False Feasible 74 (24,09%)	True Unfeasible 234 (75,91%)	308
		1055	445	

Figure 25: Confusion matrix of the “overall” prediction

		Predicted Class (ANN)		
		Feasible	Unfeasible	
True Class (OpenSees)	Feasible	True Feasible 1138 (91,12%)	False Unfeasible 111 (8,88%)	1249
	Unfeasible	False Feasible 74 (29,48%)	True Unfeasible 177 (70,52%)	251
		1212	288	

Figure 26: Confusion matrix of the prediction only in X direction (SLD + SLV)

and obtain sub-optimal solutions to the retrofitting problem. These solutions can be further optimized using a FE-based method. This allows for a faster

		Predicted Class (ANN)		
		Feasible	Unfeasible	
True Class (OpenSees)	Feasible	True Feasible 1286 (82,31%)	False Unfeasible 145 (17,69%)	1431
	Unfeasible	False Feasible 15 (24,09%)	True Unfeasible 54 (75,91%)	69
		1301	199	

Figure 27: Confusion matrix of the prediction only in Y direction (SLD + SLV)

		Predicted Class (ANN)		
		Feasible	Unfeasible	
True Class (OpenSees)	Feasible	True Feasible 1250 (93,90%)	False Unfeasible 81 (6,10%)	1331
	Unfeasible	False Feasible 69 (41,04%)	True Unfeasible 100 (58,96%)	169
		1319	181	

Figure 28: Confusion matrix of the prediction only at SLD limit state (X + Y direction)

565 design process and limits the use of computationally-expensive optimization
procedures only to further refine a restricted sub-set of approximate solutions.

		Predicted Class (ANN)		
		Feasible	Unfeasible	
True Class (OpenSees)	Feasible	True Feasible 1018 (84,47%)	False Unfeasible 187 (15,53%)	1205
	Unfeasible	False Feasible 99 (33,51%)	True Unfeasible 196 (66,49%)	295
		1117	383	

Figure 29: Confusion matrix of the prediction only at SLV limit state (X + Y direction)

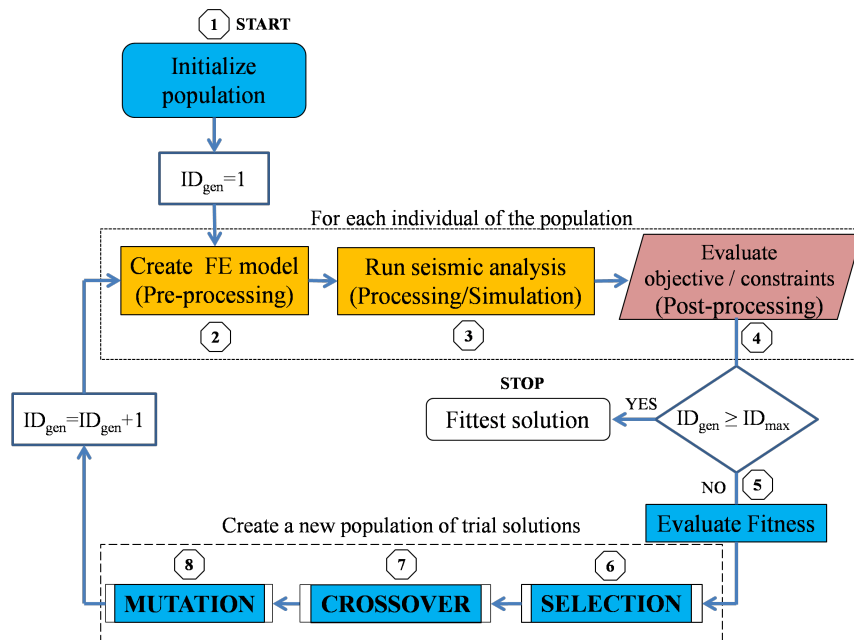


Figure 30: Flow-chart of the optimization procedure

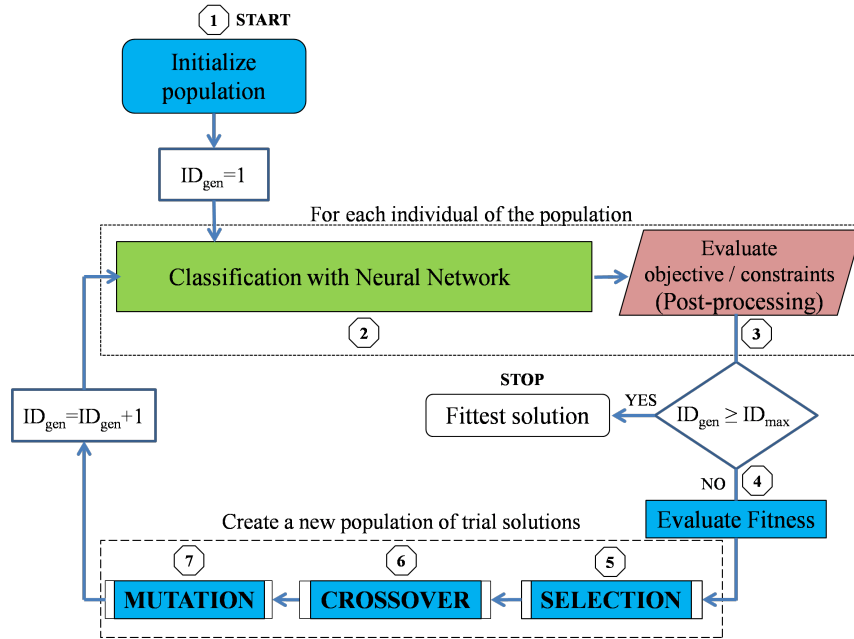


Figure 31: Flow-chart updated with the ANN-based classifier.

It is worth describing the steps of the flow-chart of Figure 30 followed by such procedure. It starts by generating a matrix representing a population of 50 individuals (candidate solutions) encoded in a chromosome like-array of design variables (genotype) which describe the retrofit intervention (installation of concentric X-shaped steel bracings), according to the same rule described in Section 5.1.1. Starting from the FE model of the as-built structure, the second subroutine reads the matrix row by row and automatically modifies the original model for adding a new steel bracing system according to the information contained in the i -th chromosome. Then, for the i -th solution the third subroutine executes a seismic analyses of the “updated” FE model by mean of the OpenSEES program to estimate the performance of the strengthened structure under the expected seismic actions. The fourth subroutine aims at evaluating both the objective (initial costs) and the performance constraints by interpreting the outcomes of the simulations. The fifth subroutine evaluates the fitness

which measures the “quality” of the candidate solution according the optimization criteria (minimum cost). Once the individuals are ranked from lowest to highest fitness value, the worst individuals are replaced with new ones through the triad of genetic operators selection-crossover-mutation. The selection applies the “survival of the fittest” principle by selecting more likely “parents” characterized by higher fitness. The crossover operator “mixes” the genetic information of the selected parents into new “offspring” solutions. The mutation modifies few, randomly selected, variables of the chromosomes achieving a local “exploration” of the design space. The trio selection-crossover-mutation keeps running until the desired number of offspring are created to replace the discarded individuals. These 8 steps are iterated until the convergence criterion is achieved. Such stopping condition is generally met after 21 hours. Specifically, through the profiling of the code the duration of each subroutine calls has been obtained: about 93% of the CPU time is used to execute the seismic analyses in OpenSees as shown in Figure 32. In fact, the search for the “best” retrofit configuration needs the execution of an huge number of seismic simulations. This process could be prohibitive due to the computational time required to perform such analyses. Since the results reported in Section confirm very good recognition capability, a possible way to enhance the computational efficiency of this procedure is the replacement of the pre-processing and processing steps (subroutines n. 2 and 3) executed with OpenSEES with the Artificial Neural Network-based meta-model able to immediately “classify” each seismic retrofit solution as either technically “feasible” or “unfeasible” only on the basis of its genotype.

This allows considerable time savings as seismic analysis is no longer necessary to assess the seismic performance of the strengthen building. For the existing building described in Section 5.1.1 a comparison has been then made

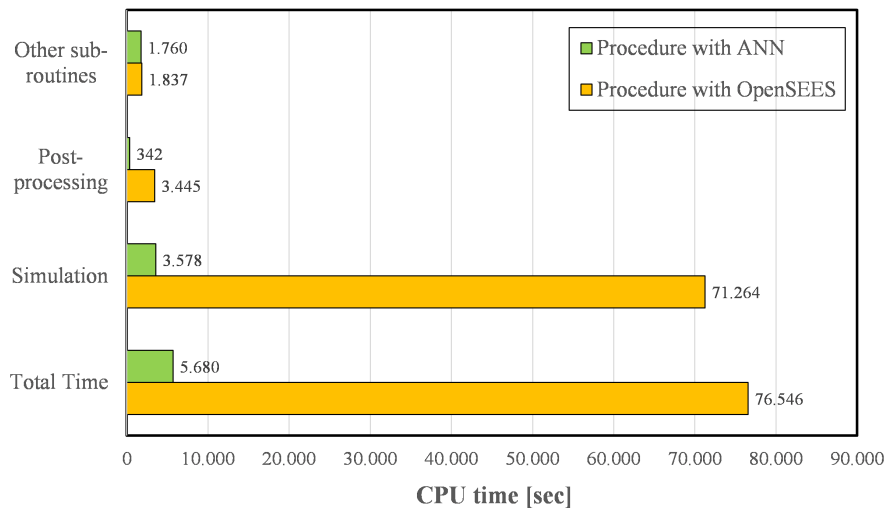


Figure 32: Time profiling of the Matlab code

between the results obtained through the original optimization procedure and the modified one with the integration of the artificial “classifier”. From the analysis of the algorithm’s convergence shown in Figure 33, it is possible to note that the objective function (initial cost) reaches almost the same minimum value (27,837€ vs 27,369€). Moreover, during the entire evolutionary process the “integrated” procedure has generated 1823 different solutions (individuals): 1668 “feasible” solutions and 155 “unfeasible” solutions. On these chromosomes a double “labeling” based both on accurate seismic analyses and rapid classification with neural network has been carried out. The result is that in 84.37% of cases the NN has been able to correctly classify the “feasible” interventions, while in 77.13% of cases it was able to recognize the class of “unfeasible” interventions. However, the time for simulations decreases from around 20 h required by the original procedure to just 1h. Consequently, the CPU time for the post-processing phase is also considerably reduced, from about 1h to 6 minutes. This, more generally, could represent a big advantage in the applications of expensive optimization procedures that require multiple “run” before accepting the

stability of the underlying heuristic and the resulting optimal solution.

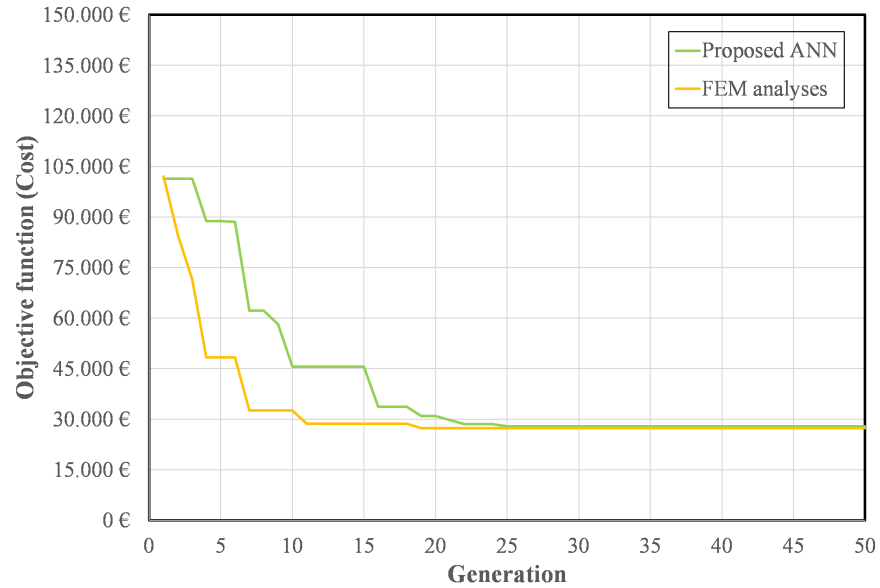


Figure 33: Comparison of the convergence curves

625 6. Conclusion

An ANN-based meta-model, which approximates the solution of more computationally expensive finite-element optimization procedure, has been proposed for a quick prediction of the technical feasibility of seismic retrofitting interventions on a RC existing building.

630 The proposed method can be used to speed-up the design process of retrofitting intervention: a neural network replaces exact optimization methods to more quickly explore the space of possible solutions and provides a sub-set of approximate solutions to the retrofitting problems, which can be further checked and optimized using exact methods. The observed benefit consists in avoiding
635 time-consuming computation for the evaluation of non-suitable solutions to the retrofitting problem, while focusing only on those that are closer to an optimal

solution. The proposed methodology thus exploits the ANN-based meta-model as a quick pre-filter for sub-optimal solutions.

Based on the results of the test, the following conclusion can be drawn: the
640 use of ANN is a valid alternative to the time-consuming seismic analyses. The
results obtained in the present study have demonstrated that it is feasible to
use ANNs to classify seismic retrofitting intervention with a good accuracy. The
results confirm that the precision is very dependent on the amount of examples
included in the training data set that should be representative enough of the
645 problem domain. However, the advantage of replacing a FEM analysis with a
Neural Network, for instance within an optimization procedure that requires a
large number of simulations, justifies the time required to train the ANN-based
meta-model.

Acknowledgments

650 This paper is part of the research project entitled “Tecniche di ottimizzazione
strutturale per l’adeguamento sismico di edifici in cemento armato” developed
under the financial support provided by the Department of Civil Engineering
(DICiv) of the University of Salerno.

References

- 655 [1] S. S. E. A. of California), Vision 2000, conceptual framework for
performance-based seismic design, Recommended Lateral Force Require-
ments and Commentary, 1996 (1996) 391–416.
- [2] D. of the Minister for Infrastructure, T. of 17 January 2018, Norme tecniche
per le costruzioni” (in italian) (2018).

- 660 [3] E. C. for Standardization (CEN), European standard en 1998-1: 2005 eurocode 8: Design of structures for earthquake resistance. part 1: General rules, seismic action and rules for buildings (2005).
- [4] E. C. for Standardization (CEN), Eurocode 8: Design of structures for earthquake resistance—part 3: Assessment and retrofitting of buildings, european standard en 1998-3: 2005 (2005).
- 665 [5] R. W. Clough, The finite element method in plane stress analysis, in: Proceedings of 2nd ASCE Conference on Electronic Computation, Pittsburgh Pa., Sept. 8 and 9, 1960, 1960.
- [6] R. Falcone, F. Carrabs, R. Cerulli, C. Lima, E. Martinelli, Seismic retrofitting of existing rc buildings: a rational selection procedure based on genetic algorithms, in: Structures, Vol. 22, Elsevier, 2019, pp. 310–326.
- 670 [7] S. K. Das, A. Kumar, B. Das, A. Burnwal, On soft computing techniques in various areas, Computer Science & Information Technology (CS & IT) 3 (2013) 59–68.
- [8] D. K. Pratihari, Soft computing: fundamentals and applications, Alpha Science International, Ltd, 2013.
- 675 [9] L. Zadeh, Foreword of the proceedings of the second international conference on fuzzy logic and neural networks, pp. xiii-xiv, Iizuka, Japan 10 (1992).
- [10] R. Falcone, C. Lima, E. Martinelli, Soft computing techniques in structural and earthquake engineering: A literature review, Engineering Structures 207 (2020) 110269.
- 680 [11] S. S. Haykin, et al., Neural networks and learning machines/simon haykin. (2009).

- 685 [12] W. J. Beni G., Swarm intelligence, in: Proceedings of the Seventh Annual Meeting of the Robotics Society of Japan., 1989, pp. 425–428.
- [13] D. E. Goldenberg, Genetic algorithms in search, optimization and machine learning (1989).
- [14] L. Zadeh, Fuzzy algorithms, Information and Control 12 (2) (1968) 94 –
690 102. doi:[https://doi.org/10.1016/S0019-9958\(68\)90211-8](https://doi.org/10.1016/S0019-9958(68)90211-8).
URL <http://www.sciencedirect.com/science/article/pii/S0019995868902118>
- [15] K. He, X. Zhang, S. Ren, J. Sun, Deep residual learning for image recognition, in: 2016 IEEE Conference on Computer Vision and Pattern Recognition (CVPR), 2016, pp. 770–778.
695
- [16] J. Kober, J. A. Bagnell, J. Peters, Reinforcement learning in robotics: A survey, The International Journal of Robotics Research 32 (11) (2013) 1238–1274. doi:10.1177/0278364913495721.
- [17] N. Strisciuglio, R. Tylecek, N. Petkov, P. Bieber, J. Hemming, E. van Henten, T. Sattler, M. Pollefeys, T. Gevers, T. Brox, R. B. Fisher, Trimbot2020: an outdoor robot for automatic gardening, in: 50th International Symposium on Robotics, VDE Verlag GmbH - Berlin - Offenbach, 2018.
700 URL http://trimbot2020.webhosting.rug.nl/wp-content/uploads/2018/04/tb_isr.pdf
- [18] M. Leyva-Vallina, N. Strisciuglio, N. Petkov, Generalized contrastive optimization of siamese networks for place recognition, CoRR abs/2103.06638 (2021).
705
- [19] X. Zhang, L. Wang, Y. Su, Visual place recognition: A survey from deep

- learning perspective, *Pattern Recognition* 113 (2021) 107760. doi:<https://doi.org/10.1016/j.patcog.2020.107760>.
- 710 [20] V. Badrinarayanan, A. Kendall, R. Cipolla, Segnet: A deep convolutional encoder-decoder architecture for image segmentation, *IEEE Transactions on Pattern Analysis and Machine Intelligence* 39 (12) (2017) 2481–2495. doi:[10.1109/TPAMI.2016.2644615](https://doi.org/10.1109/TPAMI.2016.2644615).
- 715 [21] M. Arashpour, T. Ngo, H. Li, Scene understanding in construction and buildings using image processing methods: A comprehensive review and a case study, *Journal of Building Engineering* 33 (2021) 101672. doi:<https://doi.org/10.1016/j.jobe.2020.101672>.
- [22] S. Wang, R. Clark, H. Wen, N. Trigoni, Deepvo: Towards end-to-end visual odometry with deep recurrent convolutional neural networks, in: 2017 IEEE International Conference on Robotics and Automation (ICRA), 2017, pp. 2043–2050. doi:[10.1109/ICRA.2017.7989236](https://doi.org/10.1109/ICRA.2017.7989236).
- 720 [23] J. Briot, G. Hadjeres, F. Pachet, Deep learning techniques for music generation - A survey, *CoRR* abs/1709.01620 (2017). arXiv:[1709.01620](https://arxiv.org/abs/1709.01620).
- 725 [24] S. Bengio, G. Heigold, Word embeddings for speech recognition, in: Proceedings of the 15th Conference of the International Speech Communication Association, Interspeech, 2014.
- [25] A. Ciaramella, G. Giunta, Packet loss recovery in audio multimedia streaming by using compressive sensing 10 (4) (2016) 387 – 392.
- 730 [26] S. Zafeiriou, D. Kollias, M. A. Nicolaou, A. Papaioannou, G. Zhao, I. Kotsia, Aff-wild: Valence and arousal ‘in-the-wild’ challenge, in: 2017 IEEE Conference on Computer Vision and Pattern Recognition Workshops (CVPRW), 2017, pp. 1980–1987.

- [27] A. Greco, N. Strisciuglio, M. Vento, V. Vigilante, Benchmarking deep networks for facial emotion recognition in the wild, *Multimedia Tools and Applications* (Mar 2022). doi:10.1007/s11042-022-12790-7.
- [28] A. Ciaramella, A. Staiano, G. Cervone, S. Alessandrini, A bayesian-based neural network model for solar photovoltaic power forecasting 54 (2016) 169–177.
- [29] A. Khan, A. Sohail, U. Zahoor, A. S. Qureshi, A survey of the recent architectures of deep convolutional neural networks, *Artificial Intelligence Review* 53 (8) (2020) 5455–5516. doi:10.1007/s10462-020-09825-6.
- [30] H. Adeli, Neural networks in civil engineering: 1989–2000, *Computer-Aided Civil and Infrastructure Engineering* 16 (2) (2001) 126–142.
- [31] S. Jegadesh, S. Jayalekshmi, A review on artificial neural network concepts in structural engineering applications, *Int J Appl Civ Env Eng* 1 (4) (2015) 6–11.
- [32] A. Abd-Elhamed, Y. Shaban, S. Mahmoud, Predicting dynamic response of structures under earthquake loads using logical analysis of data, *Buildings* 8 (4) (2018) 61.
- [33] S. Gholizadeh, J. Salajegheh, E. Salajegheh, An intelligent neural system for predicting structural response subject to earthquakes, *Advances in Engineering Software* 40 (8) (2009) 630–639.
- [34] N. D. Lagaros, M. Papadrakakis, Neural network based prediction schemes of the non-linear seismic response of 3d buildings, *Advances in Engineering Software* 44 (1) (2012) 92–115.
- [35] J. Estêvão, Feasibility of using neural networks to obtain simplified capacity curves for seismic assessment, *Buildings* 8 (11) (2018) 151.

- [36] J. Li, U. Dackermann, Y.-L. Xu, B. Samali, Damage identification in civil
760 engineering structures utilizing pca-compressed residual frequency response
functions and neural network ensembles, *Structural Control and Health
Monitoring* 18 (2) (2011) 207–226.
- [37] M. Vafaei, A. b. Adnan, A. B. Abd. Rahman, A neuro-wavelet technique
765 for seismic damage identification of cantilever structures, *Structure and
Infrastructure Engineering* 10 (12) (2014) 1666–1684.
- [38] K. Morfidis, K. Kostinakis, Seismic parameters' combinations for the opti-
mum prediction of the damage state of r/c buildings using neural networks,
Advances in Engineering Software 106 (2017) 1–16.
- [39] T. M. Ferreira, J. M. C. Estêvão, R. Maio, R. Vicente, The use of artificial
770 neural networks to estimate seismic damage in traditional masonry build-
ings, in: *16th European Conference on Earthquake Engineering (16ECEE)*,
2018, pp. 1–10.
- [40] K. Morfidis, K. Kostinakis, Approaches to the rapid seismic damage predic-
tion of r/c buildings using artificial neural networks, *Engineering Structures*
775 165 (2018) 120–141.
- [41] A. Calabrese, C. G. Lai, Fragility functions of blockwork wharves using
artificial neural networks, *Soil Dynamics and Earthquake Engineering* 52
(2013) 88–102.
- [42] E. Ferrario, N. Pedroni, E. Zio, F. Lopez-Caballero, Bootstrapped artificial
780 neural networks for the seismic analysis of structural systems, *Structural
Safety* 67 (2017) 70–84.
- [43] C. C. Mitropoulou, M. Papadrakakis, Developing fragility curves based

on neural network ida predictions, *Engineering Structures* 33 (12) (2011) 3409–3421.

- 785 [44] Z. Wang, N. Pedroni, I. Zentner, E. Zio, Seismic fragility analysis with artificial neural networks: Application to nuclear power plant equipment, *Engineering Structures* 162 (2018) 213–225.
- [45] A. Kaveh, Y. Gholipour, H. Rahami, Optimal design of transmission towers using genetic algorithm and neural networks, *International Journal of Space*
790 *Structures* 23 (1) (2008) 1–19. doi:10.1260/026635108785342073.
- [46] Z. Xia, S. T. Quek, A. Li, J. Li, M. Duan, Hybrid approach to seismic reliability assessment of engineering structures, *Engineering Structures* 153 (2017) 665–673.
- [47] S. M. Vazirizade, S. Nozhati, M. A. Zadeh, Seismic reliability assessment of
795 structures using artificial neural network, *Journal of Building Engineering* 11 (2017) 230–235.
- [48] P. Fajfar, M. Fischinger, N2-a method for non-linear seismic analysis of regular buildings, in: *Proceedings of the ninth world conference in earthquake engineering*, Vol. 5, 1988, pp. 111–116.
- 800 [49] F. I. du Béton (FIB), *Seismic assessment and retrofit of reinforced concrete buildings* (2003).
- [50] F. I. du Béton (FIB), *Retrofitting of concrete structures by externally bonded frps with emphasis on seismic applications* (2006).
- [51] B. Roy, *How outranking relation helps multiple criteria decision making*,
805 SEMA (Metra International), Direction Scientifique, 1972.

- [52] D.-C. Lee, B.-K. Oh, S.-W. Choi, H.-S. Park, Multi-objective optimization for performance-based seismic retrofit using connection upgrade, *International Journal of Civil and Environmental Engineering* 5 (11) (2011) 555–560.
- 810 [53] S. Wilkinson, F. J. Ying, The application of life cycle costing for building retrofit (2007).
- [54] C. Grosan, A. Abraham, Intelligent data analysis using multiple criteria decision making, in: *Proceedings of IADIS European Conference Data Mining*, Vol. 2007, Citeseer, 2007, pp. 89–94.
- 815 [55] W. S. McCulloch, W. Pitts, A logical calculus of the ideas immanent in nervous activity, *The bulletin of mathematical biophysics* 5 (4) (1943) 115–133.
- [56] D. W. Marquardt, An algorithm for least-squares estimation of nonlinear parameters, *Journal of the society for Industrial and Applied Mathematics*
820 11 (2) (1963) 431–441.
- [57] M. F. Møller, A scaled conjugate gradient algorithm for fast supervised learning, Aarhus University, Computer Science Department, 1990.
- [58] J. E. Dennis, Jr, J. J. Moré, Quasi-newton methods, motivation and theory, *SIAM review* 19 (1) (1977) 46–89.
- 825 [59] M. Riedmiller, H. Braun, A direct adaptive method for faster backpropagation learning: The rprop algorithm, in: *IEEE international conference on neural networks*, IEEE, 1993, pp. 586–591.
- [60] F. McKenna, G. L. Fenves, M. H. Scott, et al., Open system for earthquake engineering simulation, University of California, Berkeley, CA (2000).

- 830 [61] D. C. Kent, R. Park, Flexural members with confined concrete, *Journal of the Structural Division* (1971).
- [62] A. L. Yettram, H. M. Husain, Grid-framework method for plates, *Journal of the Engineering Mechanics Division* 91 (3) (1965) 53–64.
- [63] F. Taucer, E. Spacone, F. C. Filippou, A fiber beam-column element for
835 seismic response analysis of reinforced concrete structures, Vol. 91, Earthquake Engineering Research Center, College of Engineering, University of California Berkeley, 1991.
- [64] C. Eurocode, Eurocode 3: Design of steel structures-part 1-1: General rules and rules for buildings, CEN, Brussels: European Committee for
840 Standardization (2005).
- [65] D. J. Higham, N. J. Higham, *MATLAB guide*, SIAM, 2016.
- [66] A. ATC, 40 (1996) seismic evaluation and retrofit of concrete buildings, Applied technology council, report ATC-40. Redwood City (1996).
- [67] T. B. Panagiotakos, M. N. Fardis, Deformations of reinforced concrete
845 members at yielding and ultimate, *Structural Journal* 98 (2) (2001) 135–148.
- [68] C. Bishop, *Neural networks for pattern recognition*, Oxford University Press, USA, 1995.
- [69] K. Swingler, *Applying neural networks: a practical guide*, Morgan Kaufmann, 1996.
850
- [70] M. Rafiq, G. Bugmann, D. Easterbrook, Neural network design for engineering applications, *Computers & Structures* 79 (17) (2001) 1541–1552.

- [71] O. R. De Lautour, P. Omenzetter, Prediction of seismic-induced structural damage using artificial neural networks, *Engineering Structures* 31 (2) (2009) 600–606.
- [72] F. Rofooei, A. Kaveh, F. M. Farahani, Estimating the vulnerability of the concrete moment resisting frame structures using artificial neural networks, *Iran University of Science & Technology* 1 (3) (2011) 433–448.
- [73] T. K. Šipoš, V. Sigmund, M. Hadzima-Nyarko, Earthquake performance of infilled frames using neural networks and experimental database, *Engineering structures* 51 (2013) 113–127.
- [74] V. Chandwani, V. Agrawal, R. Nagar, Modeling slump of ready mix concrete using genetic algorithms assisted training of artificial neural networks, *Expert Systems with Applications* 42 (2) (2015) 885–893.
- [75] Matlab, Neural networks toolbox user guide. (2019).
- [76] R. Caruana, S. Lawrence, C. L. Giles, Overfitting in neural nets: Backpropagation, conjugate gradient, and early stopping, in: *Advances in neural information processing systems*, 2001, pp. 402–408.
- [77] M. T. Hagan, H. B. Demuth, M. Beale, *Neural network design*, PWS Publishing Co., 1997.
- [78] L. Breiman, et al., Heuristics of instability and stabilization in model selection, *The annals of statistics* 24 (6) (1996) 2350–2383.